

Quantifying Concentration Fluctuations in Binary Glass-Forming Systems by Small- and Wide-Angle X-ray Scattering

Xiao Jin, Yanhui Zhang, Jun-Qiang Wang, Juntao Huo, and Li-Min Wang*

Cite This: *J. Phys. Chem. Lett.* 2022, 13, 2205–2210

Read Online

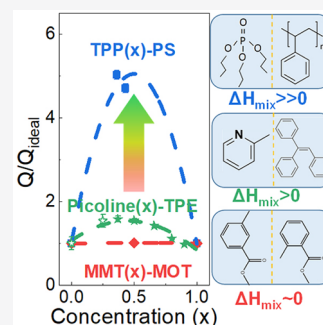
ACCESS |

Metrics & More

Article Recommendations

Supporting Information

ABSTRACT: Functionality of amorphous multicomponent systems largely depends upon the miscibility among components, especially in systems such as amorphous drugs and electrolytes. An in-depth understanding of mixing behaviors of various constituents is necessitated. Here, we applied the small- and wide-angle X-ray scattering (SWAXS) technique to monitor the mixing behaviors in three typical glass-forming binary systems imposed by varied heat of mixing. It is found that the Porod invariant (Q) determined at the glass transition temperature is remarkably enhanced as the concentration fluctuation becomes intensified. Meanwhile, the deviation of Q from the ideal mixing law is markedly weakened at elevated temperatures. The results unambiguously suggest that the degree of concentration fluctuations in mixing systems can be accurately quantified by the structural property, allowing the link to mixing thermodynamics.



The properties and performance of materials are significantly tweaked when forming mixtures or solutions with more components, especially in systems such as amorphous drugs,¹ liquid electrolytes,² and alloys,³ where serious concentration fluctuations would cause component segregation and performance degradation.^{3–5} Therefore, it is essential to have a better understanding of various behaviors in mixing systems, which is highly relevant to the structures and chemical properties of constituents. However, the knowledge for the mixing behaviors is mainly based on indirect measurements using properties such as heat of mixing ΔH_{mix} reflecting the interactions between the unlike species,^{6,7} or, dynamically, the width relaxation profile gauged by the non-exponential factor (or stretching exponent) β_{KWW} ($0 < \beta_{\text{KWW}} \leq 1$) of structural α relaxation, which is crucial to address the dynamic heterogeneity in glasses and supercooled liquids.⁸ The dynamic parameter can be obtained by fitting the α -relaxation dispersion using the Kohlrausch–Williams–Watts (KWW) function, $\phi(t) = \exp[-(t/\tau_\alpha)^{\beta_{\text{KWW}}}]$,⁹ where τ_α is the relaxation time.^{10,11} However, the quantitative relationship between the two parameters and the concentration fluctuations has not been available, and direct access to concentration fluctuations in mixing systems with higher accuracy still remains to be clarified.

For decades, the small- and wide-angle X-ray scattering (SWAXS) technique has been widely applied in many fields involving the microscopic analysis of polymers,^{12,13} liquid metals,¹⁴ glasses,^{15,16} and mesoporous materials,¹⁷ by focusing on the electron density fluctuation in nanodomains to obtain access to structural details on length scale from angstrom to micrometer.^{17,18} Thereby, considerable knowledge of amorphous materials and liquids is captured, such as the nanosize and surface morphology of polymers or proteins,^{12,13,19,20}

liquid-phase transition of alcohols,²¹ crystallization degree of CaCO_3 -saturated solutions,²² interactions of water in polymers and ethanol solutions,^{23,24} and facets and layers of amorphous materials.^{14,25,26}

Recently, the studies of deep eutectic solvent systems^{27,28} indicate that the spatial distribution of ions and interactions of electron density can be scrutinized by combining molecular dynamics simulation with SWAXS techniques. Also, the optimal extraction concentration in the extractant solvents can be determined by SWAXS signals.²⁹ The results suggest that the technique can evaluate the interactions among constituents by understanding how concentration fluctuates in mixing systems. In this paper, we apply the SWAXS technique to explore the mixing behaviors in three typical glass-forming binary systems with different concentration fluctuations, aiming at finding the way to accurately address the mixing degree of solutions via the electron density fluctuation.

Isomeric systems formed by mixing methyl *m*-toluate (MMT) and methyl *o*-toluate (MOT) represent the nearly ideal mixing systems, because our previous studies gave the maximum heat of mixing ΔH_{mix} to be as low as 11.7 J/mol³⁰ as a result of similar molecular structures and physical and chemical properties, such as polarity.³¹ The mixtures constituted by 2-picoline and triphenylethylene (TPE) are

Received: January 4, 2022

Accepted: February 28, 2022

Published: March 1, 2022



used to represent the moderately strong asymmetric systems, because the two chemicals contain similar benzene rings in structure but differ in their physical and chemical properties, like molecular size and polarity. Obvious concentration fluctuations have been detected in our recent studies using dielectric and enthalpy relaxation measurements.^{32–34} Albeit the ΔH_{mix} value of the asymmetric systems is not accessible as a result of the remarkable difference in melting points, it can be evaluated by referring to binary systems of picoline with chemicals with a structure similar to TPE. For example, ΔH_{mix} in the mixture of picoline ($x = 0.5$) and apolar *meta/ortho*-xylene is 250 J/mol,³⁵ and when increasing 10 carbon atoms in the phenyl group to arrive at 1-phenyldecane, ΔH_{mix} reaches 1200 J/mol.³⁶ It is thus expected that ΔH_{mix} between picoline and TPE is 1 order of magnitude higher than the isomeric MMT–MOT systems, reaching hundreds of joules per mole ($\Delta H_{\text{mix}} \sim 10^2\text{--}10^3$ J/mol). For an extremely strong asymmetric system, the mixtures of tripropyl phosphate (TPP)–polystyrene (PS) are the focus as a result of their tremendous difference in both structure and chemistry. The TPP molecule is polar and has a chain-like structure, while PS is an apolar polymer built by benzene ring units with a high molecular weight M_w of 2000. Two glass transition behaviors have been featured in the binary systems.³⁷ Studies of ΔH_{mix} in the mixtures of TPP with alkanes has shown extremely large values. For example, when mixed with *n*-decane of finite carbon number, ΔH_{mix} reaches 1500 J/mol.³⁸ Therefore, a very positive and large ΔH_{mix} is expected in the binary system of TPP and PS, being 2 orders of magnitude higher than the isomeric MMT–MOT systems, i.e., $\Delta H_{\text{mix}} > 10^3$ J/mol.

The SWAXS curves after denoising and smoothing are shown in panels a–c of Figure 1 for three binary systems

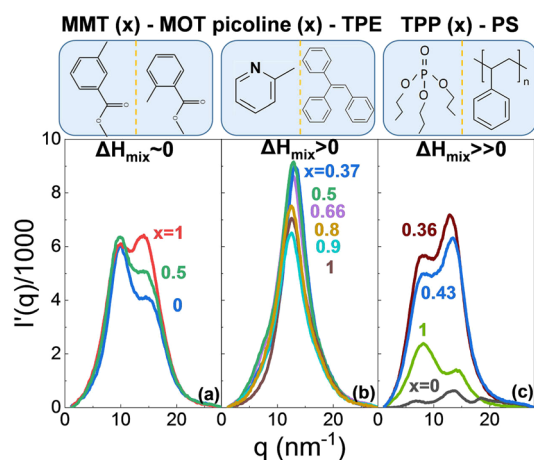


Figure 1. SWAXS curves near their glass transition temperatures of the three binary systems: (a) MMT–MOT, (b) picoline–TPE, and (c) TPP–PS. The molecular structures are shown.

MMT–MOT, picoline–TPE, and TPP–PS. The data process and original data are available in Figures S1–S4 of the Supporting Information. The mixtures were prepared according to mass fractions. The SWAXS measurements are carried out in the temperature range close to their respective glass transition temperatures (T_g), when considering the two facts that concentration fluctuations in mixtures can be markedly enhanced at T_g ^{10,11,39,40} and liquid viscosity approaches a nearly constant value of 10^{12} Pa s at T_g .^{10,11} The molecular structures of the constituents in the three systems are also

displayed in Figure 1, showing an increased degree of structural asymmetry from left to right. When the three binary systems are compared, only one scattering peak is observed in the picoline–TPE mixtures, which is probably ascribed to the rigid structure of picoline and TPE molecules, indicative of the correlations among whole molecules. In contrast, the MMT–MOT and TPP–PS systems have two and three peaks. According to earlier studies,⁴¹ the multiple peak behaviors stem from different types of intermolecular correlations and, thus, occur preferentially in the flexible molecules with polar functional groups. For the MMT–MOT system, the position and intensity of the low- q peaks are basically unchanged, while the high- q peak grows significantly with MMT, and the peak position moves toward low q . Whereas the low- q peaks correspond to the correlation generated by whole molecules, the high- q peaks can be understood in terms of the correlation caused by the ester group with a smaller coherent length. Because the methyl group in MMT is located a bit further from the ester group, the steric hindrance for the ester group is weakened (i.e., from *ortho* to *meta*), giving rise to enhanced intensity. The TPP–PS mixtures have two flexible molecules, and in particular, PS with the high molecular weight has various segmental movements as a result of its strong flexibility. The peaks correspond to the correlations with different coherence lengths.⁴²

Figure S2 of the Supporting Information gives the experimental results of picoline–TPE mixtures. The peak intensity I_{max} increases with the TPE concentration, but the peak positions change slightly. According to the relation between the coherent length D and the scattering vector q , $D = 2\pi/q$, $D \sim 0.5$ nm is determined for the picoline–TPE mixtures, which agrees well with the reported values of molecular liquids⁴¹ but is larger than those of metallic systems of 0.2–0.3 nm.^{14,27}

For the studies of small-angle X-ray scattering, Porod invariant Q is a key parameter,^{43,44} because it quantifies the fluctuation of electron density and relates to the entropy of the systems.^{43,45,46} Therefore, invariant Q is expected to reflect the concentration fluctuation at various mixing degrees. Invariant Q is defined by the mean square of excessive scattering density

$$Q = \int_0^\infty I(q)q^2 dq = \langle \rho - \bar{\rho} \rangle^2 2\pi^2 V \quad (1)$$

where $I(q)$ is the relative scattering intensity, q is the scattering vector ($q = 4\pi \sin \theta/\lambda$, where 2θ is the scattering angle and λ is the X-ray wavelength), $\langle \rho - \bar{\rho} \rangle$ or $\Delta\rho$ is the electron density difference, with $\bar{\rho}$ being the average electron density of a scattering bulk, and V is the scattering volume, which remains roughly unchanged.⁴⁴ Figure 2 shows calculated Q in terms of eq 1 using the data in Figure 1 for the three binary systems by choosing a representative $I(q)$ curve measured at specific temperatures near their T_g values. The source data and calculation process for all other concentrations are presented in Figures S2–S5 of the Supporting Information.

Panels d–f of Figure 2 show the concentration dependence of invariant Q for the mixtures. The dashed lines define ideal Q_{ideal} derived on the basis of the ideal mixing law

$$Q_{\text{ideal}} = Q_1 x + Q_2 (1 - x) \quad (2)$$

where Q_1 and Q_2 are the invariants of pure phases A and B and x is the mass fraction of phase A. Data for the crystallized samples are marked by open symbols. Early studies used the scattering peak to monitor the crystallization degree in

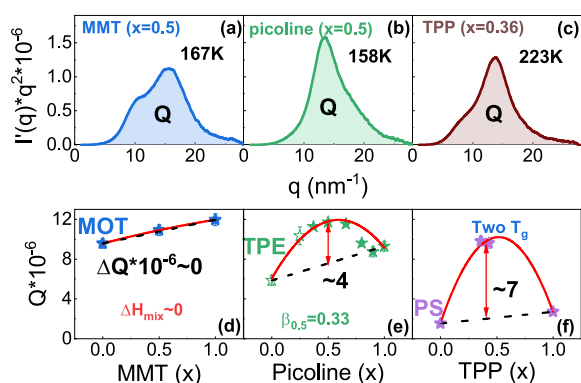


Figure 2. (a–c) Derivation of invariant Q and (d–f) concentration dependence of Q for the three systems of MMT–MOT, picoline–TPE, and TPP–PS. The dashed lines define Q_{ideal} in terms of the ideal mixing law, and the red solid lines are the binomial fitting. The open stars in panel e are from the crystallized samples.

amorphous alloys,¹⁴ polymers, and proteins,^{47,48} showing that the scattering areas do not change markedly upon crystallization, indicative of comparable invariant Q between crystalline and amorphous samples. For picoline ($x = 0$ and 0.25)–TPE, because it is highly difficult to be vitrified, invariant Q calculated from the scattering areas of the crystallized sample is used for comparison in Figure 2. It can be seen that the MMT–MOT system basically coincides with the ideal mixing line, while a large deviation occurs for both the picoline–TPE and TPP–PS mixtures, where the binomial fitting (red solid line) is used to show the degree of deviation from the ideal mixing. The largest deviation occurs in the TPP–PS system, consistent with its largest heat of mixing among the three systems.

Figure 3 presents the temperature dependence of invariant Q of picoline ($x = 0.5$ and 1)–TPE and TPP ($x = 0.36$ and 0.43)–PS systems in the glasses and supercooled liquids. The

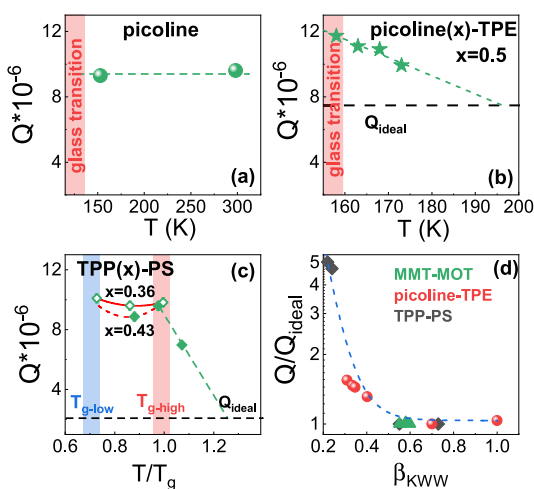


Figure 3. Temperature dependence of invariant Q for (a) pure picoline and binary (b) picoline–TPE and (c) TPP–PS mixtures. The black dashed lines stand for Q_{ideal} calculated in terms of the ideal mixing law, and the green dashed lines are the extrapolation. The relation between invariant Q normalized by Q_{ideal} and stretching exponent β_{KWW} of the structural relaxation is shown in panel d. The dielectric data of β_{KWW} comes from refs 32–34. The blue dashed line is a guide for the eye.

temperature-dependent SWAXS data and integral of eq 1 are available in Figures S6 and S7 of the Supporting Information, showing a general tendency of decreased intensity with the temperature. Above T_g , invariant Q of pure picoline changes slightly with the temperature, as shown in Figure 3a, while a rapid decrease can be seen in the picoline ($x = 0.5$)–TPE mixture, as illustrated in Figure 3b, where the extrapolation of Q gives $Q_{\text{ideal}} \sim 195$ K. For the TPP–PS ($x = 0.36$) system with two distinct T_g , it is seen in Figure 3c that invariant Q has a tendency of an initial decrease followed by an increase from low-temperature T_g to high-temperature T_g .

Concentration fluctuations in glass-forming mixtures have been understood in a quantitative manner using the dynamic stretching exponent β_{KWW} of the structural relaxation,^{8,30,32,34} largely based on the connection of β_{KWW} with dynamic heterogeneity.^{10,31,49} Figure 3d presents a plot of Q normalized by Q_{ideal} as a function of dielectric β_{KWW} for the mixtures at different temperatures and concentrations. The dielectric data of three mixtures are obtained from refs 32–34. In general, Q/Q_{ideal} decreases with β_{KWW} , spanning nearly the whole dynamics of β_{KWW} from 0.2 to 1.⁵⁰ In particular, for the system with extremely low β_{KWW} (~ 0.23),³⁴ as detected in the strongly asymmetric TPP–PS mixtures, high Q/Q_{ideal} values are achieved and then decrease exponentially until they become nearly constant.

To exhibit the deviation of invariant Q in the three systems from the ideal mixing, the concentration dependence of Q/Q_{ideal} is plotted in Figure 4. ΔH_{mix} maxima for the three

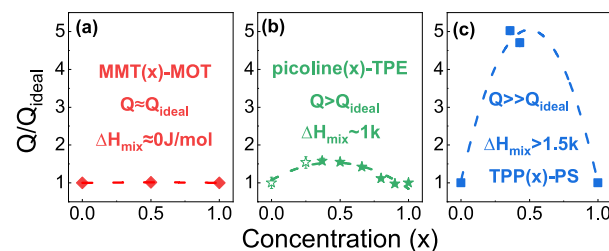


Figure 4. Concentration dependence of invariant Q normalized by Q_{ideal} for the three binary systems of (a) MMT–MOT, (b) picoline–TPE, and (c) TPP–PS. The dashed lines are from the binomial fitting.

systems are approximated by referring to the data reported in refs 30, 36, and 38. It is easily observed that the deviation is continuously enhanced, as ΔH_{mix} increases from the MMT–MOT mixtures with nearly ideal mixing to moderately asymmetric picoline–TPE and, eventually, to the extremely strongly asymmetric TPP–PS system.

On the basis of the heat of mixing ΔH_{mix} together with the stretching exponent β_{KWW} , it is confirmed that the concentration fluctuations become intensive from MMT–MOT to TPP–PS systems. The MMT–MOT mixtures are composed of isomeric molecules³³ with negligible ΔH_{mix} ³⁰ and therefore, it is not a surprise to see Q obey the ideal mixing law. In contrast, the picoline–TPE system has enhanced and positive ΔH_{mix} ^{35,36} and a marked shift of Q/Q_{ideal} from the ideal mixing line is obvious. Our recent studies of the picoline–TPE mixtures indeed revealed some unusual dynamic behaviors, such as T_g inconsistency of the dielectric and calorimetric measurements and the remarkable deviation from the relation of β_{KWW} and nonlinear factor x established by generic glass-forming liquids.³² The unusual behaviors are a direct

consequence of the large concentration fluctuation of the asymmetric systems.^{32,37,51} A large number of studies^{34,52} on the TPP–PS mixtures also verified the nature of extremely strong concentration fluctuations, featured by multiple structural relaxations and glass transitions.^{34,37,52,53}

The distinct Q deviation from the ideal mixing for the three binary systems shown in Figures 2 and 4 verifies its strong dependence of various mixing modes imposed by the increased degree of concentration fluctuations. Moreover, the correlation between Q/Q_{ideal} and β_{KWW} plotted in Figure 3d suggests how the dynamic heterogeneity and concentration fluctuation are related. In addition, at high temperatures, enhanced dynamics can be expected to lead inevitably to the weakening of concentration fluctuations.^{34,37,47} This is supported by the experimental observation, as exhibited in panels b and c of Figure 3. The close relations of Q/Q_{ideal} with β_{KWW} and ΔH_{mix} thus emphasize that the strong concentration fluctuations cause a large difference of electron density distribution, producing a high Q value shifting largely from Q_{ideal} .

Finally, the Ornstein–Zernike correlation length, which has been used widely to study the density and concentration fluctuations in solutions and polymeric blends on the basis of the calculation of the low-angle scattering data,^{21,27} is also examined in the present studies. Studies usually exhibit an inflection in the $\log I - \log q$ curves of SWAXS data at the low- q regime (typically, $q < 5 \text{ nm}^{-1}$) to address long-range density fluctuations.^{21,29} Unfortunately, no inflection point can be observed for the present three mixing systems. Note that the Ornstein–Zernike correlation length has been basically applied in complex systems, such as spinodal decomposition and liquid–liquid phase transitions,^{21,54} and thus, it might not work out in small-molecule miscible systems to analyze the concentration fluctuations.

In summary, the SWAXS signals are measured to study the concentration fluctuations in three typical glass-forming binary systems with increased difference in structures and chemical properties, addressing various concentration fluctuations. Strong concentration fluctuations are revealed in the system with extremely large and positive heat of mixing ΔH_{mix} . The strong correlations of invariant Q at varied composition and temperature with the kinetic stretching exponent and thermodynamic ΔH_{mix} are exhibited. Our results suggest that invariant Q can quantitatively characterize the degree of the concentration fluctuations in mixing systems.

■ ASSOCIATED CONTENT

SI Supporting Information

The Supporting Information is available free of charge at <https://pubs.acs.org/doi/10.1021/acs.jpcllett.2c00011>.

Additional experimental details, materials, and methods, including source data and the data processing of different mixing systems (PDF)

■ AUTHOR INFORMATION

Corresponding Author

Li-Min Wang – State Key Laboratory of Metastable Materials Science and Technology and College of Materials Science and Engineering, Yanshan University, Qinhuangdao, Hebei 066004, People's Republic of China; orcid.org/0000-0003-0484-2646; Email: limin_wang@ysu.edu.cn

Authors

Xiao Jin – State Key Laboratory of Metastable Materials Science and Technology and College of Materials Science and Engineering, Yanshan University, Qinhuangdao, Hebei 066004, People's Republic of China; orcid.org/0000-0003-3052-7543

Yanhui Zhang – State Key Laboratory of Metastable Materials Science and Technology and College of Materials Science and Engineering, Yanshan University, Qinhuangdao, Hebei 066004, People's Republic of China; orcid.org/0000-0002-7584-4705

Jun-Qiang Wang – CAS Key Laboratory of Magnetic Materials and Devices and Zhejiang Province Key Laboratory of Magnetic Materials and Application Technology, Ningbo Institute of Materials Technology and Engineering, Chinese Academy of Sciences, Ningbo, Zhejiang 315201, People's Republic of China

Juntao Huo – CAS Key Laboratory of Magnetic Materials and Devices and Zhejiang Province Key Laboratory of Magnetic Materials and Application Technology, Ningbo Institute of Materials Technology and Engineering, Chinese Academy of Sciences, Ningbo, Zhejiang 315201, People's Republic of China; orcid.org/0000-0002-2107-4979

Complete contact information is available at: <https://pubs.acs.org/doi/10.1021/acs.jpcllett.2c00011>

Notes

The authors declare no competing financial interest.

■ ACKNOWLEDGMENTS

This work was supported by the National Key R&D Program of China (Grant 2018YFA0703602), the National Natural Science Foundation of China (Grants 51871193 and 52102079), and the Natural Science Foundation of Hebei Province (Grant E2021203115).

■ REFERENCES

- (1) Duarte, D. M.; Richert, R.; Adrjanowicz, K. Frequency of the AC Electric Field Determines How a Molecular Liquid Crystallizes. *J. Phys. Chem. Lett.* **2020**, *11*, 3975–3979.
- (2) Zhao, Q.; Liu, X.; Zheng, J.; Deng, Y.; Warren, A.; Zhang, Q.; Archer, L. Designing Electrolytes with Polymerlike Glass-forming Properties and Fast Ion Transport at Low Temperatures. *Proc. Natl. Acad. Sci. U.S.A.* **2020**, *117*, 26053–26060.
- (3) Zheng, Q.; Zhang, Y.; Montazerian, M.; Gulbiten, O.; Mauro, J. C.; Zanutto, E. D.; Yue, Y. Understanding Glass through Differential Scanning Calorimetry. *Chem. Rev.* **2019**, *119*, 7848–7939.
- (4) Adrjanowicz, K.; Kaminski, K.; Tarnacka, M.; Szklarz, G.; Paluch, M. Predicting Nanoscale Dynamics of a Glass-Forming Liquid from Its Macroscopic Bulk Behavior and Vice Versa. *J. Phys. Chem. Lett.* **2017**, *8*, 696–702.
- (5) Ngai, K. L.; Valenti, S.; Capaccioli, S. Molecular Dynamic in Binary Mixtures and Polymer Blends with Large Difference in Glass Transition Temperatures of the Two Components: A Critical Review. *J. Non-Cryst. Solids* **2021**, *558*, 119573.
- (6) Tu, W.; Wang, Y.; Li, X.; Zhang, P.; Tian, Y.; Jin, S.; Wang, L.-M. Unveiling the Dependence of Glass Transitions on Mixing Thermodynamics in Miscible Systems. *Sci. Rep.* **2015**, *5*, 8500.
- (7) Kimura, T.; Ozaki, T.; Nakai, Y.; Takeda, K.; Takagi, S. Excess Enthalpies of Binary Mixtures of Propanediamine + Propanediol at 298.15 K. *J. Therm. Anal. Calorim.* **1998**, *54*, 285–296.
- (8) Duvvuri, K.; Richert, R. Binary Glass-forming Materials: Mixtures of Sorbitol and Glycerol. *J. Phys. Chem. B* **2004**, *108*, 10451–10456.

- (9) Ngai, K. L. *Glass-Forming Substances and Systems. Relaxation and Diffusion in Complex Systems. Partially Ordered Systems*; Springer: New York, 2011; pp 49–628, DOI: 10.1007/978-1-4419-7649-9_2.
- (10) Angell, C. A.; Ngai, K. L.; McKenna, G. B.; McMillan, P. F.; Martin, S. W. Relaxation in Glass Forming Liquids and Amorphous Solids. *J. Appl. Phys.* **2000**, *88*, 3113–3157.
- (11) Debenedetti, P. G.; Stillinger, F. H. Supercooled Liquids and the Glass Transition. *Nature* **2001**, *410*, 259–267.
- (12) Roe, R. J. *Methods of X-ray and Neutron Scattering in Polymer Science*; Oxford University Press: Oxford, U.K., 2000; pp 134–208.
- (13) Leite, W. C.; Weiss, K. L.; Phillips, G.; Zhang, Q.; Qian, S.; Tsutakawa, S. E.; Coates, L.; O'Neill, H. Conformational Dynamics in the Interaction of SARS-CoV-2 Papain-like Protease with Human Interferon-Stimulated Gene 15 Protein. *J. Phys. Chem. Lett.* **2021**, *12*, 5608–5615.
- (14) Li, M.; Huang, Y.; Xue, P.; Jiang, S.; Ru, W.; Yang, Z.; Yin, H.; Daisenberger, D.; Shen, H.; Sun, J. Temperature-induced Atomic Structural Evolution in a Liquid Ga-based Alloy. *Vacuum* **2019**, *170*, 108966.
- (15) Shi, W. Role of Defects in Achieving Highly Asymmetric Lamellar Self-Assembly in Block Copolymer/Homopolymer Blends. *J. Phys. Chem. Lett.* **2020**, *11*, 2724–2730.
- (16) Reibstein, S.; Wondraczek, L.; De Ligny, D.; Krolikowski, S.; Sirotkin, S.; Simon, J. P.; Martinez, V.; Champagnon, B. Structural Heterogeneity and Pressure-Relaxation in Compressed Borosilicate Glasses by in Situ Small Angle X-ray Scattering. *J. Chem. Phys.* **2011**, *134*, 204502.
- (17) Feigin, L. A.; Svergun, D. I. *Structure Analysis by Small-Angle X-ray and Neutron Scattering*; Plenum: New York, 1987; pp 14–15.
- (18) Ivanović, M. T.; Hermann, M. R.; Wójcik, M.; Pérez, J.; Hub, J. S. Small-angle X-ray Scattering Curves of Detergent Micelles: Effects of Asymmetry, Shape Fluctuations, Disorder, and Atomic Details. *J. Phys. Chem. Lett.* **2020**, *11*, 945–951.
- (19) Miyazaki, T.; Hoshiko, A.; Akasaka, M.; Shintani, T.; Sakurai, S. SAXS Studies on Structural Changes in a Poly (vinyl alcohol) Film during Uniaxial Stretching in Water. *Macromolecules* **2006**, *39*, 2921–2929.
- (20) Rambo, R. P.; Tainer, J. A. Accurate Assessment of Mass, Models and Resolution by Small-angle Scattering. *Nature* **2013**, *496*, 477–481.
- (21) Murata, K. I.; Tanaka, H. Microscopic Identification of the Order Parameter Governing Liquid–liquid Transition in a Molecular Liquid. *Proc. Natl. Acad. Sci. U.S.A.* **2015**, *112*, 5956–5961.
- (22) Van der Beek, D.; Petukhov, A. V.; Oversteegen, S. M.; Vroege, G. J.; Lekkerkerker, H. N. W. Evidence of the Hexagonal Columnar Liquid-crystal Phase of Hard Colloidal Platelets by High-resolution SAXS. *Eur. Phys. J. E* **2005**, *16*, 253–258.
- (23) Clark, G. N.; Hura, G. L.; Teixeira, J.; Soper, A. K.; Head-Gordon, T. Small-angle Scattering and the Structure of Ambient Liquid Water. *Proc. Natl. Acad. Sci. U.S.A.* **2010**, *107*, 14003–14007.
- (24) Hura, G. L.; Menon, A. L.; Hammel, M.; Rambo, R. P.; Poole, F. L.; Ii, T.; Tsutakawa, S. E.; Jenney, F. E., Jr; Classen, S.; Frankel, K. A.; Hopkins, R. C.; Yang, S.; Scott, J. W.; Dillard, B. D.; Adams, M. W. W.; Tainer, J. A. Robust, High-throughput Solution Structural Analyses by Small Angle X-ray Scattering (SAXS). *Nat. Methods* **2009**, *6*, 606–612.
- (25) Gangopadhyay, A. K.; Blodgett, M. E.; Johnson, M. L.; McKnight, J.; Wessels, V.; Vogt, A. J.; Mauro, N. A.; Bendert, J. C.; Soklaski, R.; Yang, L.; Kelton, K. F. Anomalous Thermal Contraction of the First Coordination Shell in Metallic Alloy Liquids. *J. Chem. Phys.* **2014**, *140*, 044505.
- (26) Wu, X.; Lan, S.; Wei, X.; Zhou, J.; Lu, Z.; Almer, J. D.; Wang, X. L. Elucidating the Nature of Crystallization Kinetics in Zr₄₆Cu₄₆Al₈ Metallic Glass through Simultaneous WAXS/SAXS Measurements. *Appl. Phys. Lett.* **2019**, *114*, 211903.
- (27) Malik, A.; Kashyap, H. K. Heterogeneity in Hydrophobic Deep Eutectic Solvents: SAXS Prepeak and Local Environments. *Phys. Chem. Chem. Phys.* **2021**, *23*, 3915–3924.
- (28) Busato, M.; Migliorati, V.; Del Giudice, A.; Di Lisio, V.; Tomai, P.; Gentili, A.; D'Angelo, P. Anatomy of a Deep Eutectic Solvent: Structural Properties of Choline Chloride: Sesamol 1:3 Compared to Reline. *Phys. Chem. Chem. Phys.* **2021**, *23*, 11746–11754.
- (29) Servis, M. J.; Stephenson, G. B. Mesostructuring in Liquid–Liquid Extraction Organic Phases Originating from Critical Points. *J. Phys. Chem. Lett.* **2021**, *12*, 5807–5812.
- (30) Liu, X.; Li, X.; Wang, J.; Feng, S.; Wang, L. M. Unveiling the Strong Dependence of the α -relaxation Dispersion on Mixing Thermodynamics in Binary Glass-forming Liquids. *Phys. Chem. Chem. Phys.* **2021**, *23*, 5644–5651.
- (31) Wang, L. M.; Li, Z.; Chen, Z.; Zhao, Y.; Liu, R.; Tian, Y. Glass Transition in Binary Eutectic Systems: Best Glass-forming Composition. *J. Phys. Chem. B* **2010**, *114*, 12080–12084.
- (32) Jin, X.; Li, Z.; Liu, Y.; Feng, S.; Wang, L. M. Identifying the Structural Relaxation Dynamics in a Strongly Asymmetric Binary Glass Former. *J. Chem. Phys.* **2021**, *154*, 144504.
- (33) Wang, L. M.; Tian, Y.; Liu, R.; Richert, R. Structural Relaxation Dynamics in Binary Glass-forming Molecular Liquids with Ideal and Complex Mixing Behavior. *J. Phys. Chem. B* **2010**, *114*, 3618–3622.
- (34) Jin, X.; Guo, Y.; Tu, W.; Feng, S.; Liu, Y.; Blochowicz, T.; Wang, L. M. Experimental Evidence of Co-existence of Equilibrium and Nonequilibrium in Two-glass-transition Miscible Mixtures. *Phys. Chem. Chem. Phys.* **2020**, *22*, 25631–25637.
- (35) Wilczura, H.; Kasprzycka-Guttman, T.; Megiel, E. Heats of mixing of binary mixture of pyridine bases and o-xylene. Experimental Results and Description According to the Theory. *Thermochim. Acta* **1994**, *247*, 237–243.
- (36) Wilczura, H.; Kasprzycka-Guttman, T.; Jarosz-Jarszewska, M.; Myslinski, A. The Intermolecular Interactions in Binaries: Pyridine Base+ Hydrocarbon, on the Base of Experimental Enthalpy of Mixing Data. *J. Therm. Anal. Calorim.* **1995**, *45*, 751–759.
- (37) Kahlau, R.; Bock, D.; Schmidtko, B.; Rössler, E. A. Dynamics of asymmetric binary glass formers. I. A Dielectric and Nuclear Magnetic Resonance Spectroscopy Study. *J. Chem. Phys.* **2014**, *140*, 044509.
- (38) Servis, M. J.; Wu, D. T.; Shafer, J. C. The Role of Solvent and Neutral Organophosphorus Extractant Structure in Their Organization and Association. *J. Mol. Liq.* **2018**, *253*, 314–325.
- (39) Tu, W.; Ngai, K. L.; Paluch, M.; Adrjanowicz, K. Dielectric Study on the Well-Resolved Sub-Rouse and JG β -Relaxations of Poly (methylphenylsiloxane) at Ambient and Elevated Pressures. *Macromolecules* **2020**, *53*, 1706–1715.
- (40) Qiao, A.; Bennett, T. D.; Tao, H.; Krajnc, A.; Mali, G.; Doherty, C. M.; Thornton, A. W.; Mauro, J. C.; Greaves, G. N.; Yue, Y. A Metal-Organic Framework with Ultrahigh Glass-Forming Ability. *Sci. Adv.* **2018**, *4*, No. eaao6827.
- (41) Lajovic, A.; Tomsic, M.; Fritz-Popovski, G.; Vlcek, L.; Jamnik, A. Exploring the Structural Properties of Simple Aldehydes: A Monte Carlo and Small-Angle X-ray Scattering Study. *J. Phys. Chem. B* **2009**, *113*, 9429–9435.
- (42) Bergfeldt, A.; Rubatat, L.; Brandell, D.; Bowden, T. Poly(benzyl methacrylate)-Poly[(oligo ethylene glycol)methyl ether methacrylate] Triblock-Copolymers as Solid Electrolyte for Lithium Batteries. *Solid State Ionics* **2018**, *321*, 55–61.
- (43) Koch, M. H.; Vachette, P.; Svergun, D. I. Small-Angle Scattering: A View on the Properties, Structures and Structural Changes of Biological Macromolecules in Solution. *Q. Rev. Biophys.* **2003**, *36*, 147–227.
- (44) Ciccariello, S.; Goodisman, J.; Brumberger, H. On the Porod Law. *J. Appl. Crystallogr.* **1988**, *21*, 117–128.
- (45) Laggner, P.; Paudel, A. Density Fluctuations in Amorphous Pharmaceutical Solids. Can SAXS Help to Predict Stability? *Colloids Surf., B* **2018**, *168*, 76–82.
- (46) Li, Z. H. A Program for SAXS Data Processing and Analysis. *Chin. Phys. C* **2013**, *37*, 108002.
- (47) Ran, S.; Fang, D.; Zong, X.; Hsiao, B. S.; Chu, B.; Cunniff, P. M. Structural Changes during Deformation of Kevlar Fibers via on-line Synchrotron SAXS/WAXD Techniques. *Polymer* **2001**, *42*, 1601–1612.

(48) Xiong, B.; Lame, O.; Chenal, J. M.; Rochas, C.; Seguela, R.; Vigier, G. Amorphous Phase Modulus and Micro–Macro Scale Relationship in Polyethylene via in Situ SAXS and WAXS. *Macromolecules* **2015**, *48*, 2149–2160.

(49) Richert, R.; Gabriel, J. P.; Thoms, E. Structural Relaxation and Recovery: A Dielectric Approach. *J. Phys. Chem. Lett.* **2021**, *12*, 8465–8469.

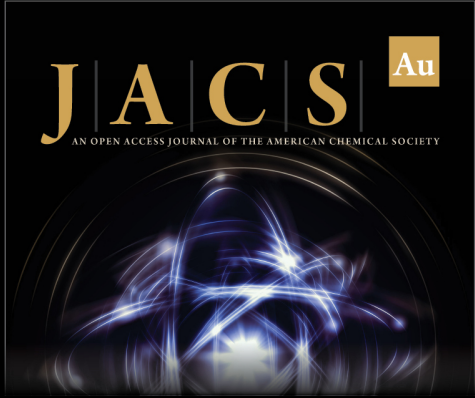
(50) Wang, L. M.; Richert, R. Primary and Secondary Relaxation Time Dispersions in Fragile Supercooled Liquids. *Phys. Rev. B* **2007**, *76*, 064201.

(51) Jin, X.; Wang, L. M. Relaxation Dynamics in Multicomponent Glass Formers with Adjustable Concentration Fluctuations. *J. Non-Cryst. Solids: X* **2021**, *11–12*, 100072.


(52) Valenti, S.; Capaccioli, S.; Ngai, K. L. Contrasting Two Different Interpretations of the Dynamics in Binary Glass Forming Mixtures. *J. Chem. Phys.* **2018**, *148*, 054504.


(53) Körber, T.; Krohn, F.; Neuber, C.; Schmidt, H. W.; Rössler, E. A. Reorientational Dynamics of Highly Asymmetric Binary Non-polymeric Mixtures—A Dielectric Spectroscopy Study. *Phys. Chem. Chem. Phys.* **2021**, *23*, 7200–7212.


(54) Herkt-Maetzky, C.; Schelten, J. Critical Fluctuations in a Binary Polymer Mixture. *Phys. Rev. Lett.* **1983**, *51*, 896–899.



JACS Au
AN OPEN ACCESS JOURNAL OF THE AMERICAN CHEMICAL SOCIETY

 Editor-in-Chief
Prof. Christopher W. Jones
Georgia Institute of Technology, USA

Open for Submissions 

pubs.acs.org/jacsau  ACS Publications
Most Trusted. Most Cited. Most Read.